DOE/ER/04694--T2

DOE/ER/04694--T2

DE84 000471

Proton Transfer and Unimolecular Decay in the Low-Energy-Reaction Dynamics of H_3O^+ with Acetone

W. R. Creasy and J. M. Farrar*

Department of Chemistry
University of Rochester
Rochester, N.Y. 14627

* Alfred P. Sloan Foundation Fellow, 1981-1985

DISCLAIMER

Abstract

The title reaction has been studied at collision energies of 0.83 eV and 2.41 eV. Direct reaction dynamics have been observed at both energies and an increasingly high fraction of the total energy appears in product translation as the collision energy increases. This result is consistent with the concept of "induced repulsive energy release", which becomes more effective as trajectories sample the corner of the potential energy surface. At the higher collision energy, the protonated acetone cation undergoes two unimolecular decay channels: C-C bond cleavage to CH_3CO^+ and CH_4, and C-O bond cleavage to $C_3H_5^+$ (presumably to allyl cation) and H_2O. The CH_3CO^+ channel, endothermic relative to ground state protonated acetone cations by 0.74 eV, appears to liberate 0.4 eV in relative product translation while the $C_3H_5^+$ channel, endothermic by 2.17 eV, liberates only 0.07 eV in relative translation. These results are discussed in terms of the location on the reaction coordinate and magnitudes of potential energy barriers to 1,3-hydrogen atom shifts which must precede the bond cleavage processes.

Introduction

The hydronium ion, H_3O^+, plays an important role in many chemical systems. In the oxygen-rich region of flames, H_3O^+ is the most abundant ionic species.[1,2] The ion, along with hydrated forms, $H_3O^+(H_2O)_n$, is important in atmospheric chemistry as one of the predominant ionic species in the troposphere.[3] The H_3O^+ ion has been observed to be a very effective proton donor in the gas phase,[4-6] and it is also, of course, the predominant acidic species in most aqueous solutions.

Despite the importance of the H_3O^+ ion, however, few detailed dynamical studies of its chemistry have been performed. Futrell et al.[7] studied reactions (1) and (2) at collision energies of 0.65 to 4.99 eV, using a crossed ion-neutral beam apparatus.

$$H_3O^+ + D_2O \longrightarrow HD_2O^+ + H_2O \qquad (1)$$

$$H_3O^+ + D_2O \longrightarrow H_2DO^+ + HDO \qquad (2)$$

These investigators found that at high energies, reaction (1) was described well by the modified spectator stripping model,[8] but at 0.65 eV, observation of multiple proton and deuteron transfers in reaction (2) suggested the formation of a persistent complex. Other gas phase studies of H_3O^+ have been conducted by Bohme et al.[4,6] using the flowing afterglow technique, and by Hiraoka[5] using mass spectrometry. These studies showed that proton transfer of H_3O^+ to many neutrals is generally rapid, with rates approaching the Langevin limit in numerous cases.

In previous work from this laboratory, we have studied the reactions of HCO^+ [9-11] and H_3O^+ [12] with water, methanol and ethanol in a crossed beam apparatus, and have observed the unimolecular decomposition products of the protonated alcohols. In all cases, the proton transfer reactions of both ions

were direct stripping processes, followed by partial decomposition of metastable parent ions which live many rotational periods.

Reactions of H_3O^+ [6] and HCO^+ [13] with acetone have been observed by Bohme et al. In neither case was decomposition of the resulting protonated acetone observed at 300°K, even though energetically allowed decomposition processes are accessible. However, decomposition of the acetone molecular cation has been observed by McAdoo and Witiak,[14] and by Lifshitz and Tzidony,[15] both using metastable mass spectrometry. The decomposition occurs predominantly through reaction (3a) for the keto isomer of the ion, and the products

$$CH_3\overset{O^+}{\overset{\|}{C}}CH_3 \longrightarrow CH_2CO^+ + CH_4 \qquad (3a)$$

$$CH_2=\overset{OH^+}{\overset{|}{C}}CH_3 \longrightarrow CH_3\overset{O^+}{\overset{\|}{C}}CH_3 \longrightarrow CH_3CO^+ + CH_3 \qquad (3b)$$

show a very small (.01 eV) kinetic energy release. Lifshitz and Tzidony also found that the enol decomposition proceeds through a 1,3 hydrogen atom shift followed by loss of methyl radical from the keto tautomer shown in reaction (3b). The transition state for the enol-keto isomerization should be "tight",[16] occurring over a large barrier. Bohme et al.[6,13] used similar reasoning to explain their failure to observe decomposition of protonated acetone formed in their flowing afterglow apparatus because of the low probability of the 1,3 hydrogen shift over the tight transition state.

In this study, we have performed a dynamical study of the proton transfer reaction (4) using a crossed beam apparatus at relative kinetic energies of 0.83 and 2.41 eV:

$$H_3O^+ + (CH_3)_2C=O \longrightarrow (CH_3)_2C=OH^+ + H_2O \qquad \Delta H = -1.28 \text{ eV} \qquad (4)$$

We have also observed two decomposition channels of the protonated acetone cation, shown in reactions (5) and (6):

$$(CH_3)_2C{=}OH^+ \longrightarrow CH_3CO^+ + CH_4 \qquad \Delta H = +0.74 \text{ eV} \qquad (5)$$

$$\longrightarrow CH_2CHCH_2^+ + H_2O \qquad \Delta H = +2.17 \text{ eV} \qquad (6)$$

These reaction products were studied at a collision energy of 2.41 eV, and appear to proceed through 1,3 hydrogen atom shifts. The heats of formation used to calculate the energetics are summarized in Table 1, and the energy relationships among the reactants, the protonated parent ion product, and its unimolecular decay products are shown in Figure 1.

Experimental

The crossed beam apparatus used in this study has been described in detail in the literature.[17] The H_3O^+ ions are prepared in an electron impact ion source using a few percent H_2O in H_2 gas according to the following chemical ionization reactions:

$$H_2^+ + H_2 \longrightarrow H_3^+ + H \quad (7)$$

$$H_3^+ + H_2O \longrightarrow H_3O^+ + H_2 \quad (8)$$

We estimate that the total pressure in the ionization region is between 0.01 and 0.1 torr. The ions are focused, mass selected, and decelerated to the desired energy, and have a FWHM energy and angular spread of 0.3 eV and 2° respectively. Beam currents range from 2×10^{-10} to 1×10^{-9} A. As we have discussed in other work from our laboratory,[12] the H_3O^+ ions produced in this manner have substantial vibrational excitation, with a measurable population having excitation energy in excess of 1.3 eV.

The neutral beam is formed by bubbling H_2 through 0° C acetone and supersonically expanding the mixture through a 0.1 mm nozzle into a differentially pumped chamber, where the beam is collimated and modulated at 150 Hz with a tuning fork chopper. Following this chamber, the beam enters the main collision region, maintained at 5×10^{-7} torr by a trapped oil diffusion pump. The scattered products are energy analyzed, mass filtered and counted by a multichannel scaler synchronized with the beam modulation under control of a minicomputer. A typical experiment consists of measuring laboratory fluxes at 6 to 10 angles, at 50 different energies per laboratory scattering angle, each energy bin having a fixed energy width ranging from 0.04 to 0.06 eV.

Typical count rates for detection of $(CH_3)_2C{=}OH^+$ were approximately 50 to 100 counts per second. This large signal rate compares favorably with previous proton transfer experiments using the present apparatus.[9-12] For the

dissociation reactions (5) and (6), however, product ions were only detected at approximately 1 to 3 cps, after subtraction of background counts. This rate is near the lower limit of detection for this apparatus, since the background count rate is often 2 cps. The measured energy distributions for unimolecular decay were noisy and were smoothed graphically prior to deconvolution. Although the gross features of the energy and flux distribtuions are quite reliable, some small oscillations in the resultant barycentric fluxes are spurious, and were ignored in our interpretation of the data.

Results

The data are analyzed in the manner described in previous publications.[17] The data are transformed into the center of mass reference frame with the correct Jacobian where they are deconvoluted from the ion and neutral beam velocity distributions using a program developed by Siska.[18] The fluxes, $I_{c.m.}(u,\theta)$, can be plotted as a polar plot in the variables u, the barycentric speed, and θ, the barycentric scattering angle. Product translational energy and angular distributions can be obtained by integration over the fluxes as indicated in the following equations:

$$P(E_T') = \sum_j \frac{1}{u} I_{c.m.}(u,\theta_j)\sin\theta_j$$

$$g(\theta) = \sum_k I_{c.m.}(u_k,\theta)$$

It was necessary to determine the velocity of the seeded acetone beam empirically; by adjusting the reactant acetone velocity until the barycentric angular distribution for proton transfer was symmetric about the relative velocity vector, we determined that the neutral velocity corresponded to a seeded gas mixture composed of approximately 7.5% acetone in H_2 gas. This concentration implies that the carrier gas was not saturated with acetone vapor at 0° C, although the beam conditions were readily reproduced from day to day.

The proton transfer reaction was studied at two collision energies. The barycentric polar flux contour map for the experiment performed at a relative collision energy of 0.83 eV is shown in Figure 2, the corresponding plot at 2.41 eV shown in Figure 3. In both cases, the product peaks very sharply in the backward direction relative to the incoming H_3O^+ ion, corresponding to direct abstraction of the proton by the incoming acetone molecule. This behavior is similar to that observed in our previous studies of proton transfer from HCO^+ and H_3O^+ to alcohols.[9-12]

The product translational energy distributions for these energies are shown in Figure 4. It is difficult to estimate the total energy of the system, since we have not been able to determine the average internal energy of the H_3O^+ ions; in our work on proton transfer from hydronium to alcohols,[12] we have determined that a significant fraction of the ions (a few percent) have as much as 1.3 eV of vibrational excitation. Accordingly, the total available energy is indicated on these plots assuming 1.3 eV of vibrational excitation in the reagent ions. Also indicated on the 2.41 eV plot is the minimum threshold energy for dissociation by reactions (5) and (6), computed by assuming that the H_3O^+ reagents are in their ground vibrational state. Note that a substantial fraction of products appear to have sufficient internal energy to dissociate. The appearance of these apparently superexcited products indicates that the H_2O product carries a significant amount of internal excitation. The branching ratios for unimolecular decay give a ratio of 1.0:0.04:0.04 for $(CH_3)_2C{=}OH^+$: CH_3CO^+:$C_3H_5^+$, with estimated uncertainties of 25%.

The spectator stripping (SS) energy is also shown on both plots. As our previous studies of proton transfer have shown, the most probable energy is near the SS point at low energy, but moves above it as the energy increases. The small dip near the top of the distribution for the 0.83 eV experiment is probably spurious, arising from coarse angular spacing in the measured flux distributions.

The barycentric polar flux distributions for the two dissociation channels are shown in Figures 5 and 6. The behavior of the two channels is quite different, a point which will be elaborated upon later. As we have discussed previously,[10,19] it is not possible to determine the velocities of three particles involved in the scattering and unimolecular decay by measuring only one ionic decay fragment. We previously used a method which assumes that the

unimolecular decay takes place with respect to the new centroid moving with the nascent parent ion. The fragment distribution must then be symmetric about the barycentric scattering angle $\pi/2$ with respect to the barycentric coordinate system of the decaying parent, assuming that the parent is sufficiently long-lived relative to a rotational period.

The kinetic energy distributions found by adjusting the relative translational energy of the decaying parents until the angular distribution of the fragment is symmetric about $\pi/2$, or, for CH_3CO^+, until the peak in the barycentric angular distribution shifts from the forward to the backward direction, are shown in Figure 7. The distribution for CH_3CO^+ in the top panel of Figure 7 peaks at about 0.4 eV and is very broad, with significant probability up to 1.3 eV. This distribution was found assuming that the nascent parent ion has translational energy of 3.6 eV prior to dissociation. At a collision energy of 2.41 eV, parent ions formed by proton transfer from vibrationally cold H_3O^+ lie 2.9 eV above the threshold for CH_3CO^+ formation, so the observation that the nascent decaying parents have 3.6 eV of translational energy indicates that the parents must be formed by reactant ions which are vibrationally excited. Figure 5 shows that the peak of the CH_3CO^+ flux distribution appears at the edge of the map, corresponding to the limiting viewing angle of our detector. The actual peak in the flux distribution may be out of the observation range of our instrument, so the most probable kinetic energy release inferred from these measurements is only a lower bound. With a total available energy of approximately 5.0 eV accessible to the reagents, 3.6 eV of kinetic energy release between the departing protonated acetone and its H_2O partner indicates that 1.4 eV is available to the unimolecular decay process; the most probable kinetic energy of 0.4 eV corresponds to 35% of the available energy.

Such kinetic energy release is significantly greater than one would expect from statistical considerations. As we discuss below, the CH_3CO^+ fragments may be the result of a "direct" reaction involving protonation on a methyl carbon, or decay of a parent ion in a time short compared to a rotational period. In these cases, the daughter CH_3CO^+ distribution would not necessarily be symmetric, and the kinetic energy release would be larger than computed using the previously described method.

The energy distribution of $C_3H_5^+$ products in the lower panel of Figure 7, in contrast, peaks at less than 0.1 eV and falls off more rapidly. The most satisfactory kinematic fit to these data suggests that the decaying parents have approximately 2.1 eV in translation. Since parent ions formed from vibrationally cold H_3O^+ at a collision energy of 2.4 eV lie only 1.5 eV above the threshold for $C_3H_5^+$ formation, the appearance of 2.1 eV in relative translation of the parent also indicates that the ions we observe result from protonation of acetone by vibrationally excited H_3O^+. The kinetic energy of 2.1 eV in initial translation of the parent is quite reliable, within the context of the single Newton diagram kinematic analysis, because the entire distribution of $C_3H_5^+$ daughter lies within the viewing range of our detector. With 5.0 eV available to the reagents, the disposal of 2.1 eV in relative translation of the primary parents leaves 2.9 eV to be distributed in the unimolecular process producing $C_3H_5^+$. The fact that the kinetic energy distribution peaks at 0.07 eV, approximately 3% of the total available energy, is in qualitative accord with the notion that one vibrational mode of the 27 of protonated acetone becomes the translational reaction coordinate for the dissociation.

Discussion

As we noted previously for the proton transfer reaction (4), the peak of the energy distributions moves above the spectator stripping energy as the collision energy is increased. It is not surprising that the spectator stripping model does not work well for a system that is this complicated, but it is useful to have a model which explains this trend qualitatively. As described by rate constant models such as the average dipole orientation (ADO) model of Bowers et al.[20] which is rather successful at predicting capture rate constants, the most important long range forces between ions and neutrals are ion-dipole and ion-induced dipole forces. One would expect that the reactants should gain translational energy as they approach under the influence of these attractive forces, and lose translational energy as they depart. For H_2O and $(CH_3)_2C{=}O$, the dipole moments are 1.84 and 2.85 D, respectively, and the polarizabilities are 1.45 and 6.11 $Å^3$ respectively.[21] When the reactants approach, the H_3O^+ ion will interact with the dipole moment and polarizability of the acetone neutral, giving larger forces than the departing H_2O neutral and $(CH_3)_2C{=}OH^+$ ion. Therefore, a net gain in translational energy in the departing product should result.

At the higher collision energy, the long range forces should play less of a role in governing the disposal of translational energy. The transfer of a proton between two relatively heavy groups can be described by motion on a potential energy surface with a small value of the skew angle β. Induced repulsive energy release[22] may result on a potential energy surface when a trajectory with high translational excitation samples the "corner" of the surface where both the breaking bond and the newly forming bond are compressed. Such trajectories result in the products entering the exit valley with the incident

translational energy partitioned primarily into product translation. This effect is most pronounced at high collision energies where any vibrational excitation in the reagents is small in comparison with translation. All of our studies of proton transfer from H_3O^+ and HCO^+ exhibit this dynamical induced repulsive energy release, enhancing the product translation at high kinetic energies.

The energy level diagram of Figure 1 shows that the exothermicity of the initial proton transfer reaction is energetically, although not necessarily dynamically, sufficient to yield the CH_3CO^+ product without vibrational excitation or hyperthermal kinetic energies in the reagents. The translational energy distribution for parent ion reaction products at a collision energy of 2.41 eV peaks near 3.2 eV, at a total energy of approximately 5.0 eV. The lower panel of Figure 3 indicates that the threshold for CH_3CO^+ production from vibrationally "cold" reagent ions coincident with formation of vibrationally cold H_2O molecules occurs at a translational energy of 3.0 eV. Observation of stable parent ions below this translational threshold is consistent with the formation of H_2O with vibrational excitation. The area under the $P(E_T')$ curve for $E_T' < 3.0$ eV represents the maximum fraction of H_2O products with vibrational energy in excess of the zero point energy. Inspection of the lower panel of Figure 4 indicates that approximately half of the H_2O products may be vibrationally excited. No protonated acetone products are formed below a translational energy of 0.2 eV; such products formed at their dissociation threshold would appear in concert with H_2O products with at least 2.8 eV of vibrational excitation. If H_2O carries away no vibrational excitation in the protonation of

acetone at 2.4 eV collision energy, the most probable internal excitation of the parent cation is the total available energy of 5.0 eV minus the most probable translational energy of 3.2 eV. The resultant 1.8 eV assigned to internal excitation of the protonated acetone suggests that a majority of those products would have sufficient energy to decay to CH_3CO^+, even if a fairly large exit channel barrier were present. This argument indicates that H_2O vibrational excitation occurs with high probability, reducing the internal excitation of protonated acetone. The translational energy distribution thus indicates that the initial proton transfer reaction channels significant vibrational excitation into the H_2O product, stabilizing the protonated acetone product relative to dissociation to CH_3CO^+. This effect is reasonable in terms of the structural differences between H_2O and H_3O^+. Since some rearrangement is necessary upon loss of H^+, the H_3O^+ ground vibrational state should have a higher Franck-Condon overlap with excited H_2O vibrational states. The failure to observe the CH_3CO^+ product in the thermal energy studies conducted by Bohme et al.[6] undoubtedly reflects the channeling of vibrational excitation into the H_2O product. However, the higher energy experiments reported in the present work indicate clearly that the lowest dissociation channel proceeds with liberation of a large amount of kinetic energy, consistent with a large exit channel barrier. If the barrier to dissociation to CH_3CO^+ products exceeds 0.54 eV, CH_3CO^+ from dissociation of parent ions produced by reaction of vibrationally cold H_3O^+ at thermal collision energy is energetically unfavorable.

The translational energy of the present experiments provides a means of surmounting this barrier but the dynamics of the initial protonation reaction create only a small population of parent ions with sufficient energy to dissociate. The experimental evidence suggests a rather large (>0.5 eV) exit channel barrier for reaction (5).

Reaction (6), involving the elimination of H_2O after an initial 1,3 hydrogen atom shift, is a much more endothermic process than the methane elimination reaction. As shown in Figure 6, the flux distribution peaks within the viewing range of our instrument, and kinematic analysis indicates that the decaying parents have approximately 2.1 eV of translational energy prior to decomposition. Of the 2.9 eV available for the decay process to allyl cation, less than 0.1 eV appears as relative translation, qualitatively consistent with a statistical distribution of energy in the precursor parent ions. In mechanistic terms, elimination of H_2O to yield allyl cation requires that a hydride ion migrate from the methyl carbon to the carbonyl oxygen, the site of the initial excitation. Energy that was initially deposited in the new O-H bond must flow into a C-H oscillator before the elimination of H_2O can occur. This process shows quite clearly that statistical intramolecular vibrational energy flow plays a vital role in the production of allyl cations.

This situation contrasts with the high kinetic energy release of reaction (5), yielding CH_3CO^+, indicative of non-statistical behavior. Formation of acetyl cations from protonated acetone requires that the proton transferred to the acetone molecule migrate to a methyl group prior to elimination. If the proton is originally attached to the carbonyl oxygen atom, much of the excitation deposited in that O-H oscillator may be required to overcome the barrier to migration. This implies that the parent ion may not be long-lived relative to a rotational period, since the energy may not have time to randomize.

Alternatively, as Bohme et al.[6] have suggested, reaction (5) may be a high energy, direct reaction in which acetone is protonated by H_3O^+ directly on a methyl carbon and decays immediately. Since the total energy of the system lies approximately 3 eV above the CH_3CO^+ threshold, the lifetime of possible protonated acetone parents could be quite short in either case, making the decay indistinguishable from a direct mechanism. Therefore, it seems unlikely that the parent ions live long enough to decay with forward-backward symmetry, making the energy release in Figure 7 a lower limit, and the parent barycentric energy an upper limit. Either proposed mechanism could scatter products preferentially in the forward direction relative to the neutral acetone, in agreement with the observations from Figure 5.

The argument in the preceding paragraph suggests that the unimolecular decay channels (5) and (6) behave in qualitatively different manners. Although both channels may require a 1,3 hydrogen atom shift prior to decay, a process which is normally thermally forbidden[23] and thus should involve a large barrier, CH_3CO^+ production manifests the barrier as high kinetic energy release, while $C_3H_5^+$ production does not. Moreover, the very high kinetic energy imparted to those parent cations which ultimately decompose to CH_3CO^+, as well as the high kinetic release in the decay itself, suggest dynamical peculiarities for this channel. The experiments of Lifshitz and Tzidony[15] on the decay of metastable acetone cations and their interpretations are instructive for the present work. The decay of the enol form of the acetone cation to CH_3 and $C_2H_3O^+$ observed in that work is mechanistically similar to the decay of protonated acetone to CH_4 and CH_3CO^+ studied in the present work. Metastable studies conducted with deuterated compounds indicate that a disproportionately high fraction of the decays occur with large kinetic energy release (0.3 eV) when the emitted methyl group contains the enol hydrogen. In direct analogy, the elimination

of CH_4 from protonated acetone requires a 1,3 hydrogen atom shift to a methyl carbon; the magnitude of the most probable kinetic energy release for this decomposition is at least 0.4 eV. This mechanistic similarity provides evidence that the formation of CH_4 and CH_3CO^+ by reaction (5) proceeds by a 1,3 hydrogen atom shift in protonated acetone, followed by subsequent decay.

The low kinetic energy release in the elimination of H_2O suggests that the reaction coordinate for dissociation does not contain an appreciable exit channel barrier, although a 1,3 hydrogen atom shift must occur before the parent ion decomposes. This observation suggests that the isomerization may pass through a "tight" transition state to yield a local minimum on the reaction coordinate in which two hydrogen atoms are bound to the oxygen. This species may then dissociate via a "loose" transition state with no exit channel barrier, to the $C_3H_5^+$ product, accompanied by a water molecule. The species at the local minimum cannot be measured directly, since it has the same mass as the protonated acetone. However, it has a protonated enol structure, which one may expect to be stable. This interpretation is consistent with the decay of the enol form of the acetone cation, in which a 1,3 hydrogen atom shift must occur, but kinetic energy release measurements indicate no exit channel barrier. In the case of acetone, the intermediate isomerized species is the keto form of the cation; kinetic energy release studies by Mintz and Baer[24] on internally state-selected acetone cations corresponding to this species, which decay by the same mechanism, indicate the absence of an exit channel barrier.

Figure 8 shows a schematic reaction coordinate for the dissociation processes indicating the exit channel barriers and the total energy accessible to the reagents. The formation of $C_3H_5^+$ may involve isomers other than the lowest energy allyl form; after H_2O elimination from the rearranged protonated acetone parent cation, the resultant methyl vinyl isomer, $CH_3CCH_2^+$, must

undergo an additional 1,2 hydrogen atom shift to form the allyl cation, which is 0.2 [25] to 0.5 [26] eV more stable. The present experiments cannot distinguish between these two isomers. The absence of an exit channel barrier suggests the possibility that the 1,2 shift occurs in concert with the C-O bond cleavage.

Conclusion

In summary, the proton transfer reaction to form protonated acetone appears to be direct at the collision energies studied and partitions an increasingly high fraction of the available energy in product translation as the collision energy increases. This observation is consistent with enhanced induced repulsive energy release as reactive trajectories reach the "corner" of the potential energy surface more efficiently at high energies. The parent ion exhibits two decay channels at 2.41 eV collision energy in which the vibrational excitation of the H_3O^+ reagent plays an important role. The acetyl cation, CH_3CO^+, is formed with rather high (>0.4 eV) kinetic energy release. This high recoil energy is indicative of an exit channel barrier, possibly arising from a 1,3 hydrogen atom shift preceding C-C bond cleavage, although one cannot rule out protonation of the methyl carbons as a direct mechanism for this product. In contrast, the formation of $C_3H_5^+$, presumed to be the allyl cation, appears to proceed in the absence of an exit channel barrier in excess of the endothermicity. We suggest that a 1,3 hydrogen atom shift from a methyl carbon to the carbonyl oxygen occurs, yielding a local minimum on the potential energy surface, from which C-O bond cleavage occurs through a "loose" transition state. The mechanistic complexity of these unimolecular decay channels, the nature of the bound intermediates along the reaction coordinate, and the presence and magnitudes of exit channel barriers suggest that theoretical calculations of the potential energy surfaces would be enlightening.

Acknowledgments

We acknowledge support of this research by the U. S. Department of Energy. W. R. C. thanks the University of Rochester for a Sherman Clarke Fellowship.

References

1. D.K. Bohme, in "Kinetics of Ion-Molecule Reactions", P. Ausloos, Ed., Plenum, New York, 1979, p. 323.

2. B.S. Fialkov and N.D. Shcherbakov, Russ. J. Phys. Chem., 54, 1513 (1980).

3. E.E. Ferguson, in "Kinetics of Ion-Molecule Reactions", P. Ausloos, Ed., Plenum, New York, 1979, p. 377.

4. R.S. Hensworth, J.D. Payzant, H.I. Schiff, and D.K. Bohme, Chem. Phys. Lett., 26, 417 (1974).

5. K. Hiraoka, Int. J. Mass Spectrom. Ion Phys., 27, 139 (1979).

6. G.I. Mackay, S.D. Tanner, A.C. Hopkinson, and D.K. Bohme, Can J. Chem., 57, 1518 (1980).

7. P.W. Ryan, C.R. Blakley, M.L. Vestal, and J. H. Futrell, J. Phys. Chem., 84, 561 (1980).

8. M.L. Vestal, A.L. Wahrhaftig, and J.H. Futrell, J. Phys. Chem., 80, 2892 (1976).

9. J.E. Moryl and J.M. Farrar, J. Phys. Chem., 86, 2016 (1982).

10. J.E. Moryl and J. M. Farrar, J. Phys. Chem., 86, 2020 (1982).

11. J.E. Moryl, W.R. Creasy, and J.M. Farrar, J. Phys. Chem., 87, 1954 (1983).

12. J.E. Moryl, W.R. Creasy, and J.M. Farrar, J. Chem. Phys., to be published.

13. S.D. Tanner, G.I. Mackay, A.C. Hopkinson, and D.K. Bohme, Int. J. Mass Spectrom. Ion Phys., 29, 153 (1979).

14. D.J. McAdoo and D.N. Witiak, J. Chem. Soc. Perkin Trans. II, 1981, 770.

15. C. Lifschitz and C. Tzidony, Int. J. Mass Spectrom. Ion Phys., 39, 181 (1981).

16. See, for example, G.M. Wieder and R.A. Marcus, J. Chem. Phys., 37, 1835 (1962).

17. R.M. Bilotta, F.N. Preuninger, and J.M. Farrar, J. Chem. Phys., 73, 1637 (1980).

18. P.E. Siska, J. Chem. Phys., 59, 6052 (1973).

19. R.M. Bilotta and J.M. Farrar, J. Phys. Chem., 85, 1515 (1981).

20. L. Bass, T. Su, W.J. Chesnavich, and M.T. Bowers, Chem. Phys. Lett., 34, 119 (1975); T. Su and M.T. Bowers, J. Chem. Phys., 58, 3027 (1973).

21. E.W. Rothe and R.B. Bernstein, J. Chem. Phys., 31, 1619 (1959).

22. A.M.G. Ding, L.J. Kirsch, D.S. Perry, J.C. Polanyi, and J.L. Schreiber, Faraday Disc. Chem. Soc., 62, 267 (1973).

23. R.B. Woodward and R. Hoffman, "The Conservation of Orbital Symmetry", Academic, New York, 1971.

24. D.M. Mintz and T. Baer, Int. J. Mass Spectrom. Ion Phys., 25, 39 (1977).

25. D.H. Aue and M.T. Bowers, in "Gas Phase Ion Chemistry", M.T. Bowers, Ed., Academic Press, New York, 1979, Vol. 2, Chapter 9.

26. D.H. Aue, W.R. Davidson, and M.T. Bowers, J. Amer. Chem. Soc. 98, 6700 (1976).

Table 1

Heats of Formation

H_3O^+	143 kcal mole^{-1} [a]
$(CH_3)_2C{=}O$	-51.5 [b]
$(CH_3)_2C{=}OH^+$	119 [c]
H_2O	-57.0 [b]
CH_3CO^+	152 [b]
CH_4	-15.99 [d]
$C_3H_5^+$	226 [e]

[a] M.A. Haney and J.L. Franklin, J. Chem. Phys., 50, 2028 (1969).

[b] H.M. Rosenstock, K. Draxl, B.W. Steiner, and J.T. Herron, J. Phys. Chem. Ref. Data, Suppl. 1, 6 (1977).

[c] Computed from the proton affinity of acetone, 194.6 kcal mole^{-1}, reported by R. Yamdagni and P. Kebarle, J. Am. Chem. Soc., 98, 1320 (1976).

[d] D.R. Stull and H. Prophet, "JANAF Thermochemical Tables". Natl. Stand. Ref. Data Ser., Natl. Bur. Stand., No. 27 (1971).

[e] F.P. Lossing, Can J. Chem., 50, 3973 (1972).

Figure Captions

Figure 1: Energy level diagram for reactants, parent ions, and unimolecular decay daughter ions.

Figure 2: Barycentric polar flux contour map for $(CH_3)_2COH^+$ production at 0.83 eV. The Newton diagram and location of the SS point are indicated. Barycentric and lab coordinate origins denoted "CM" and "O" respectively.

Figure 3: Barycentric polar flux contour map for $(CH_3)_2COH^+$ production at 2.41 eV. The Newton diagram and location of the SS point are indicated. Barycentric and lab coordinate origins denoted "CM" and "O" respectively.

Figure 4: Translational energy distributions for reaction products at the two collision energies indicated. Arrows denote the SS energy and total available energy for both distributions. Thresholds for formation of $C_3H_5^+$ and CH_3CO^+ assuming the initial H_2O product is vibrationally cold are indicated by arrows marked "A" and "M" respectively.

Figure 5: Barycentric polar flux contour map for CH_3CO^+ production at a relative translational energy of 2.41 eV. The Newton diagram is indicated. Barycentric and lab coordinate origins denoted "CM" and "O" respectively.

Figure 6: Barycentric polar flux contour map for $C_3H_5^+$ production at 2.41 eV translational energy. The Newton diagram is indicated. Barycentric and lab coordinate origins denoted "CM" and "O" respectively.

Figure 7: Barycentric energy distributions for unimolecular decay products relative to barycenter of decaying parent. See text for explanation.
Upper panel: CH_3CO^+ production at 2.41 eV collision energy, parent translational energy of 3.6 eV.
Lower Panel: $C_3H_5^+$ production at 2.41 eV collision energy, parent translational energy of 2.1 eV.

Figure 8: Schematic reaction coordinate for unimolecular decay channels; barrier heights are qualitative only.

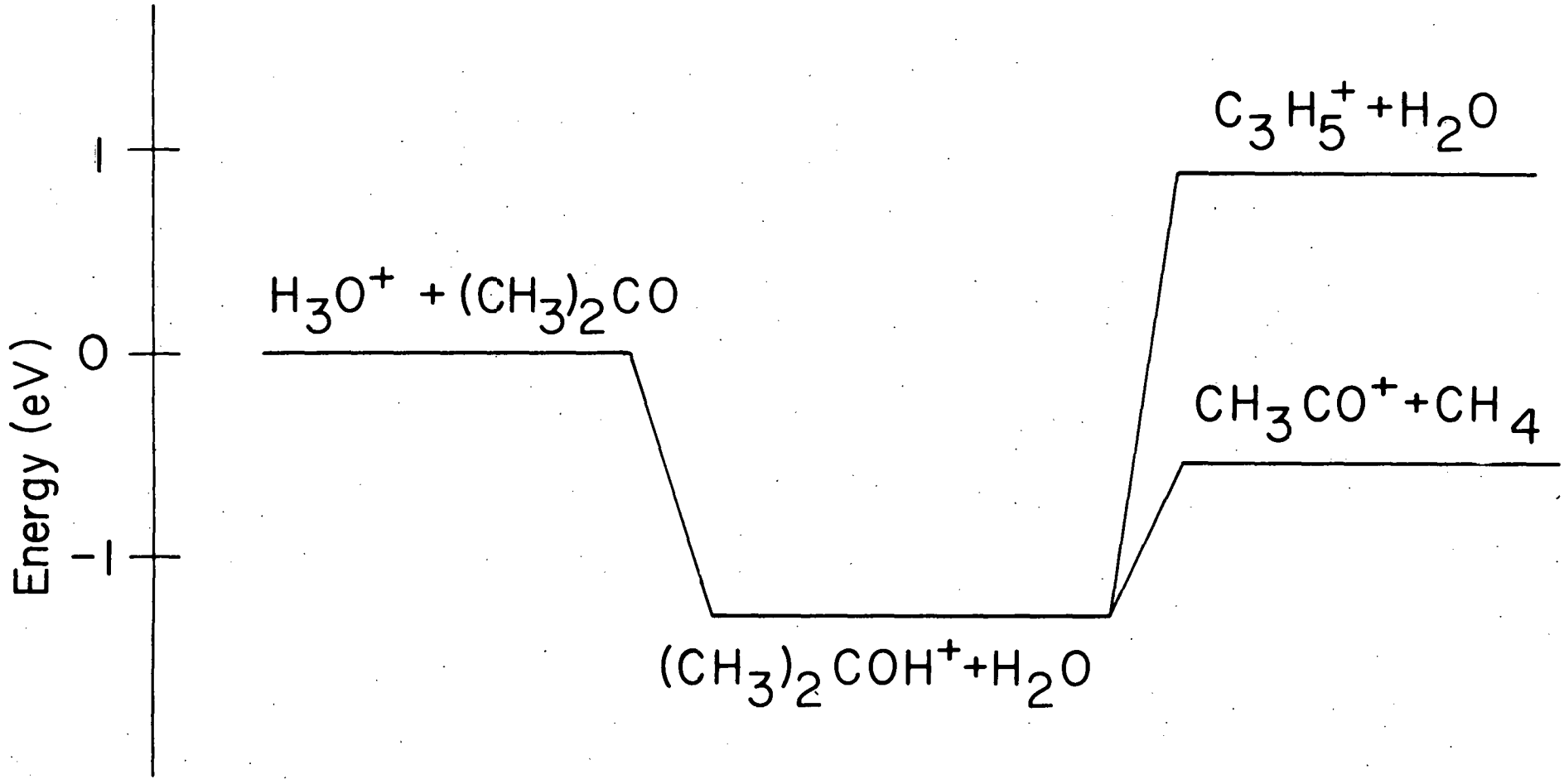

Fig. 1

$$H_3O^+ + (CH_3)_2CO \longrightarrow \underline{(CH_3)_2COH^+} + H_2O$$

$E_{rel} = 0.83$ eV

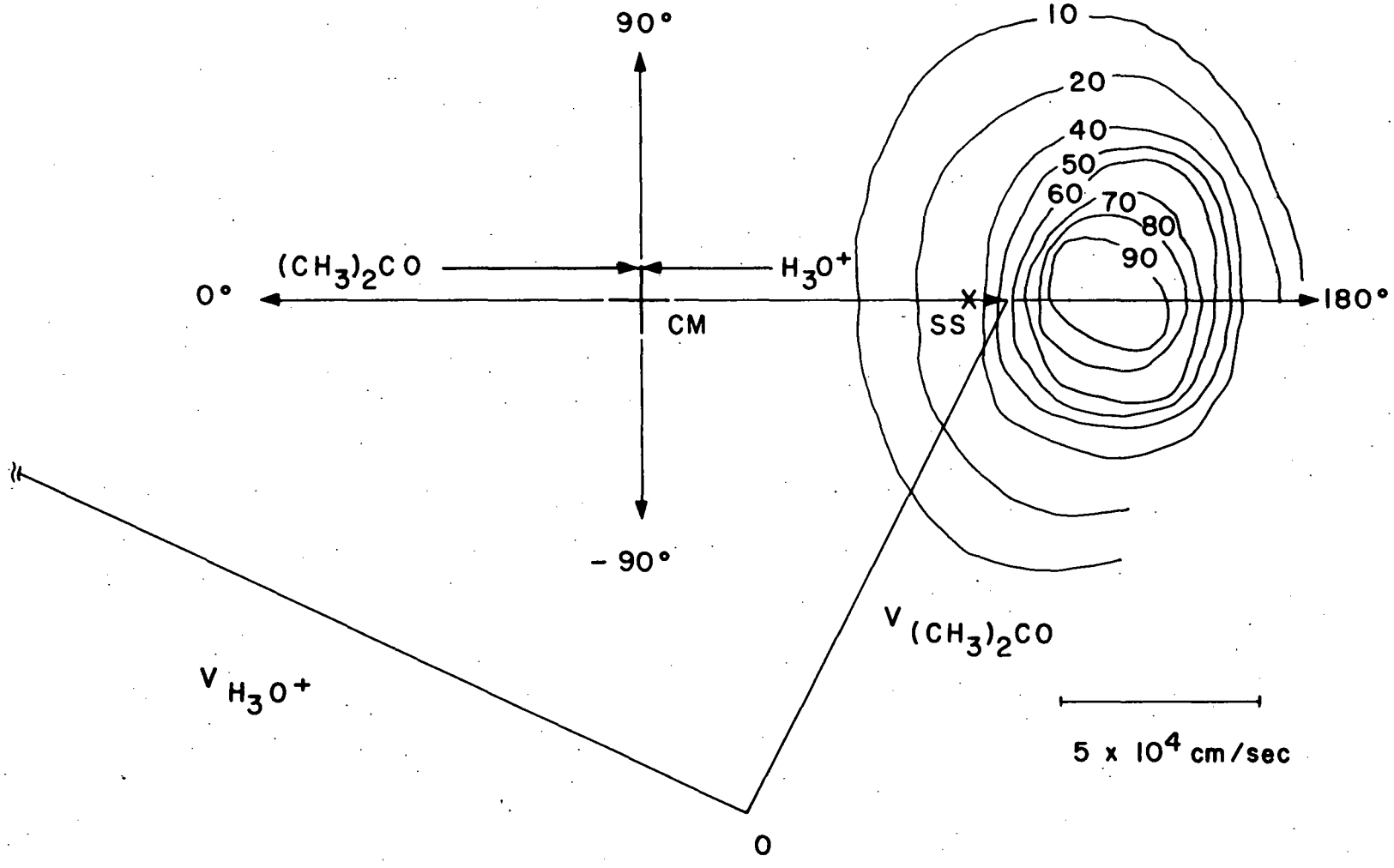

$$H_3O^+ + (CH_3)_2CO \longrightarrow \underline{(CH_3)_2COH^+} + H_2O$$

$E_{rel} = 2.41$ eV

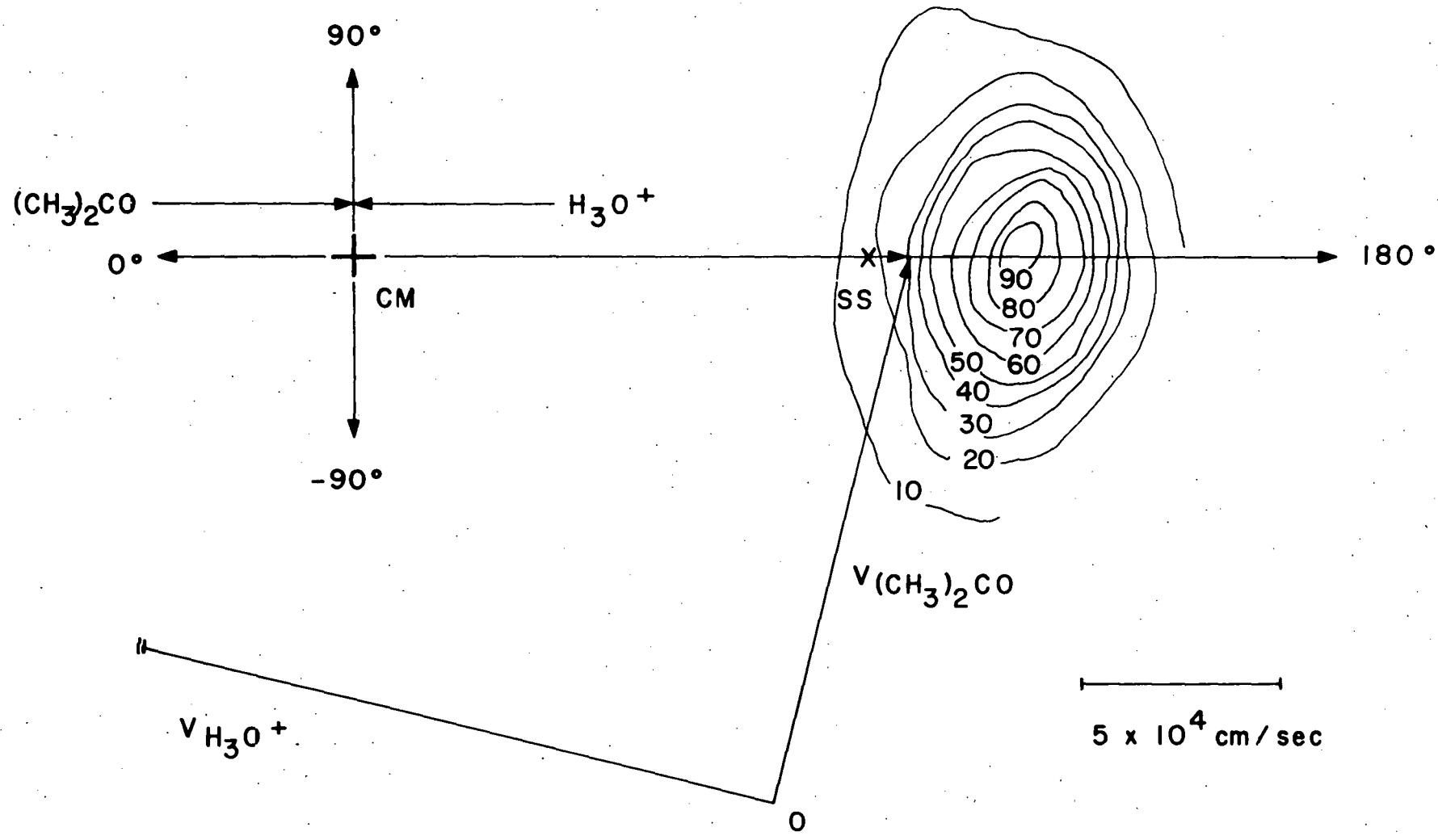

Fig 3

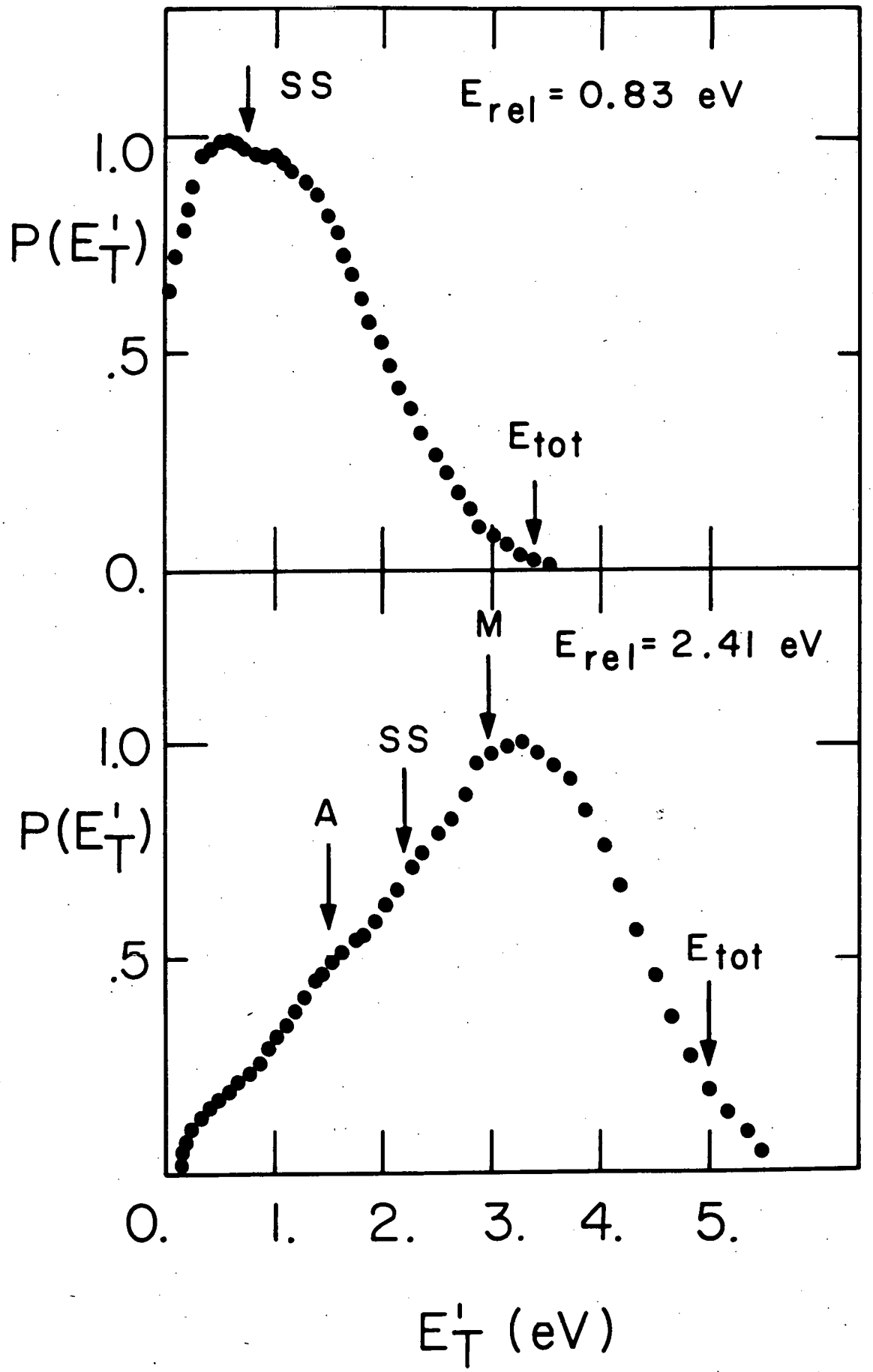
SS
E_{rel} = 0.83 eV
1.0
$P(E'_T)$
.5
E_{tot}
0.
M
E_{rel} = 2.41 eV
1.0
SS
A
$P(E'_T)$
.5
E_{tot}
0.
1.
2.
3.
4.
5.
E'_T (eV)

Fig. 4

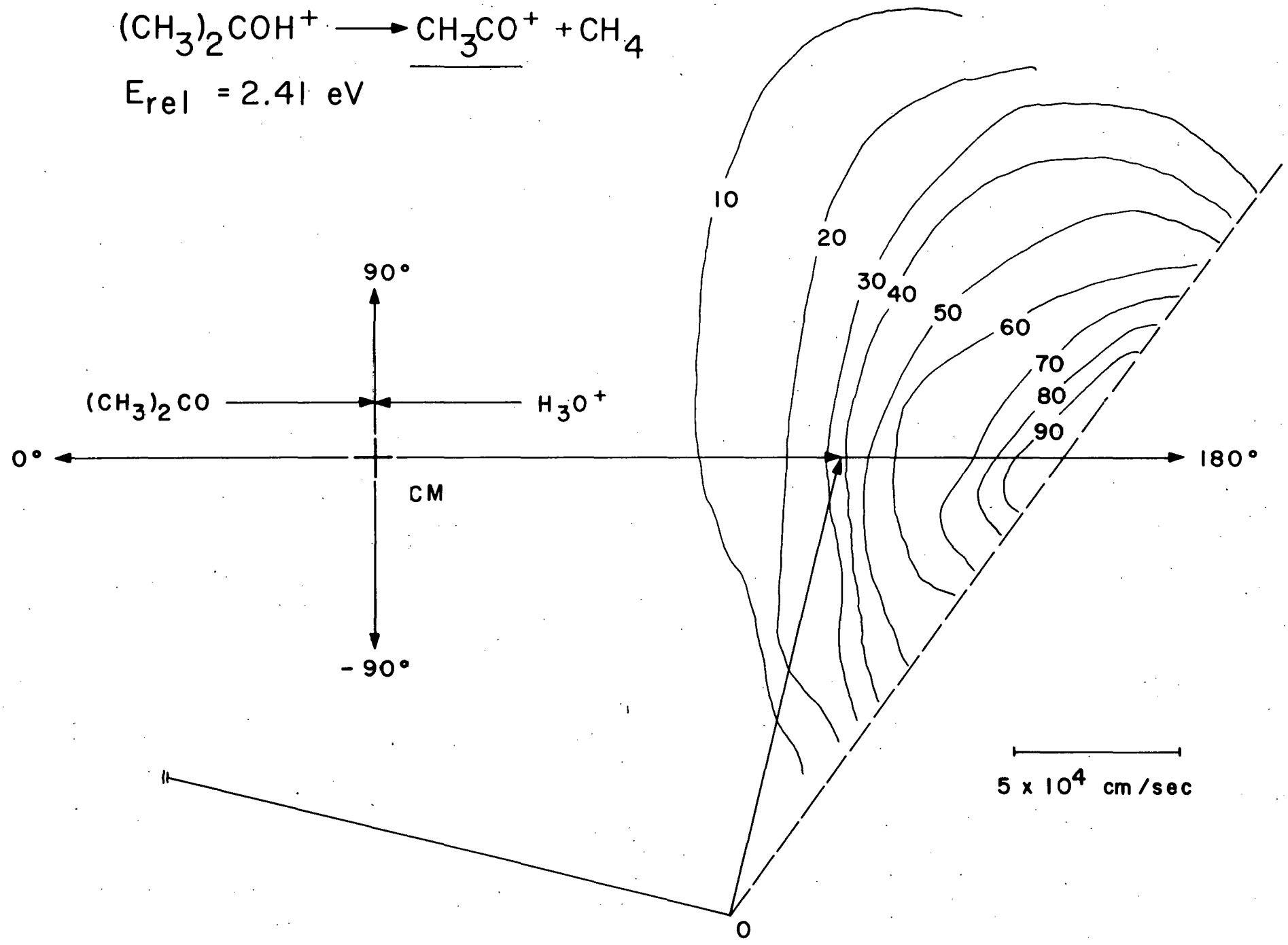
$(CH_3)_2COH^+ \longrightarrow CH_3CO^+ + CH_4$
E_{rel} = 2.41 eV
10
20
30
40
50
60
70
80
90
90°
$(CH_3)_2CO$
H_3O^+
0°
180°
CM
-90°
0
5×10^4 cm/sec

Fig. 5

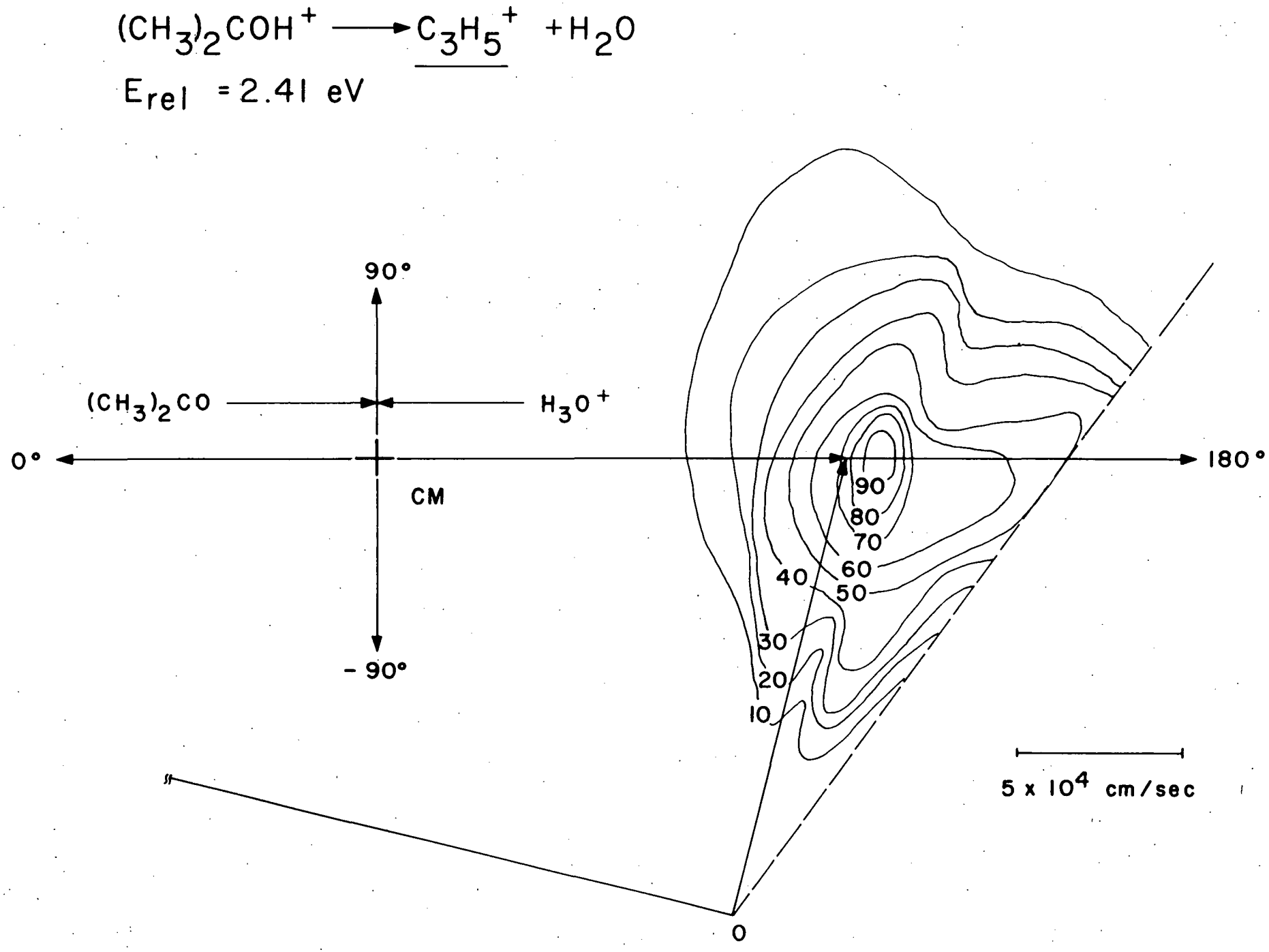
$(CH_3)_2COH^+ \longrightarrow C_3H_5^+ + H_2O$
E_{rel} = 2.41 eV
90°
$(CH_3)_2CO$
H_3O^+
0°
180°
CM
- 90°
90
80
70
60
50
40
30
20
10
0
5 x 10^4 cm/sec

Fig. 6

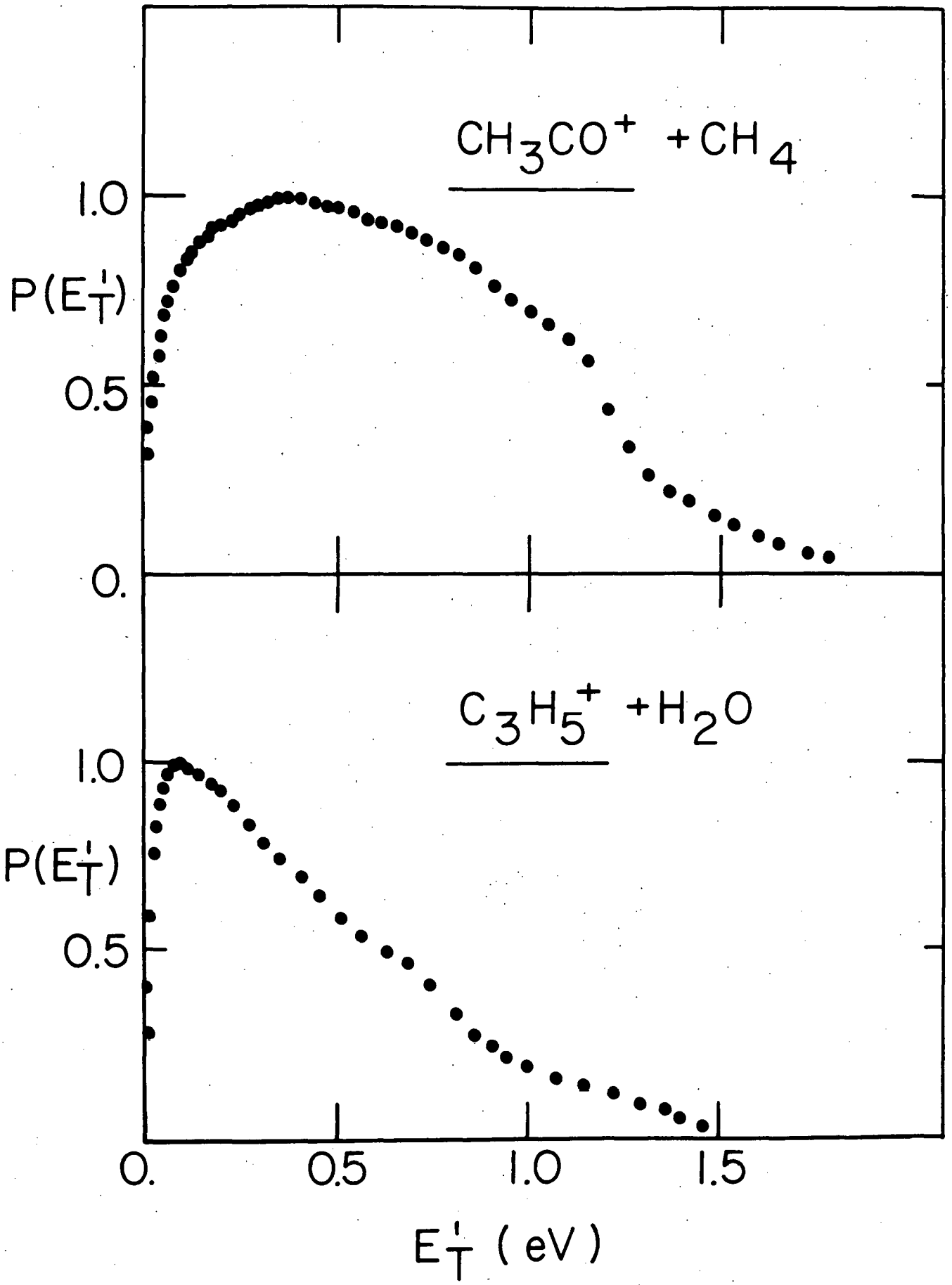

Fig. 7

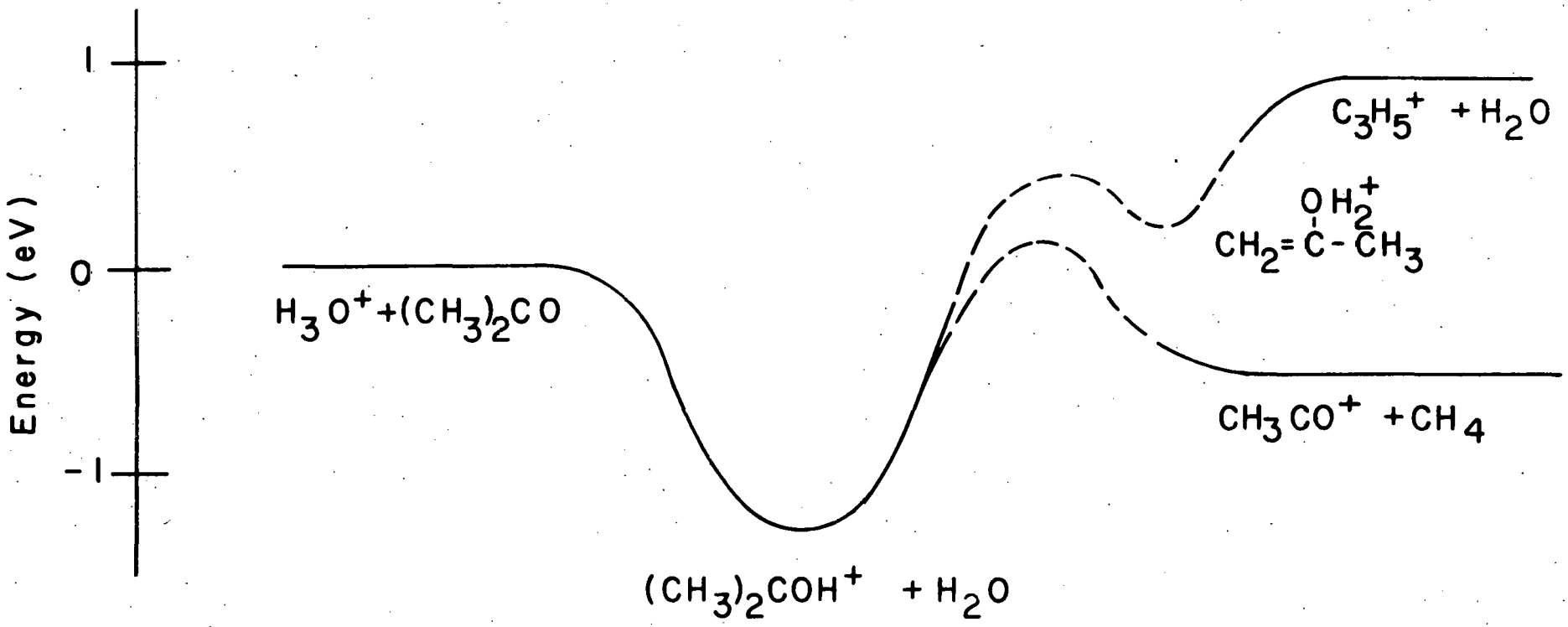
Energy (eV)
1
0
-1
$H_3O^+ + (CH_3)_2CO$
$(CH_3)_2COH^+ + H_2O$
$C_3H_5^+ + H_2O$
$CH_2=\overset{\overset{OH_2^+}{|}}{C}-CH_3$
$CH_3CO^+ + CH_4$

Fig. 8